Contributed paper

OPTO-ELECTRONICS REVIEW **11**(2), 113–117 (2003)

Kinetics of photoluminescence of porous silicon studied by photo-luminescence excitation spectroscopy and time-resolved spectroscopy

Z. ŁUKASIAK*, P. DALASIŃSKI, and W. BAŁA

Faculty of Physics, Astronomy and Informatics, N. Copernicus University,
5 Grudziądzka Str., 87-100 Toruń, Poland

Photoluminescence (PL) spectra and excitation spectra (PLE) (under steady-state conditions), time resolved spectra (PL-TRS) and decay curves of photoluminescence (PL-DC) in micro- and nanosecond range (under pulsed operation) at different temperatures (10 K-room) on anodically etched boron – doped silicon are presented. PLE shows that visible PL is excited by light from UV region. PL and PL-TRS exhibit multiband structure and can be decomposed as a sum of few Gaussians. PL-DCs have multiexponential shape. Relaxation times depend on wavelength of the observation. To explain our results we assumed a model in which the multibarrier structure is formed by larger Si crystallites or wires (quantum well) surrounded by Si crystallites with diameters in the nanometer range (barrier region). The visible photoluminescence originates from radiative recombination between discrete energy levels in a quantum well.

Keywords: porous silicon, photoluminescence, decay times, time resolved spectra, excitation spectra.

1. Introduction

One of the recent remarkable trends in semiconductor physics is the interaction between physics, materials sciences and technology. The advanced semiconductor structures like superlattices demonstrated by Esaki and Tsu as long ago as in 1969 [1] clearly represent that direction. Today, in solid-state physics and materials sciences, many researchers are discovering and producing more complex structures and composites that have unique physical properties. Nanometer-size semiconductor crystallites are subset of the notable examples of complex structures. Optical and electronic properties of nanocrystallites have potential application for becoming novel and future devices.

Silicon is the basis for the majority of integrated electronic devices. However, due to the indirect band gap in its electronic structure, bulk silicon exhibits very weak luminescence. Therefore Si has not been a useful material for manufacturing of active optical devices, e.g., light emitting diodes or laser diodes. Over the past several years, there has been a rising level of research work focused on the goal of improving the efficiency of light emission from Si based materials through various schemes to produce artificial structures. Porous silicon (PSi) has attracted much attention as a new optoelectronic material since the observation of its efficient visible photoluminescence at room temperature [2]. A number of experimental [3] and theoretical studies [4] have been reported so far in order to clarify origin of light emission by PSi layers. Model of such phenomena in which the visible emission originates from electron-hole recombination between discrete energy levels inside the quantum wells formed by bulk silicon regions separated by nanoscale silicon particles (nanocrystallites) was first proposed by Canham [2]. This model called "quantum confinement model" is widely accepted, but some of its aspects are still matter of controversy and need further investigations. Some reports suggest that photoluminescent properties of PSi make it attractive as a highly sensitive gas sensor [5,6] or biomedical tag [7]. After 12 years of research no fast LEDs based on PSi have been demonstrated. The main problem with PSi is its natural slow speed of operation. Detailed knowledge about kinetic processes inside PSi skeleton (mainly radiative and nonradiative recombination) may help to obtain structures with better parameters.

2. Experimental

The porous silicon samples were prepared by electrochemical anodisation of p-type epitaxial layer deposited on low resistivity p substrate (0.01 Ω cm) under a current density of 10 mA/cm^2. An epitaxial structure as a starting material assures good uniformity and reproducibility of luminescence spectra. As an electrolyte the HF acid (40% in H_2O) diluted in isopropyl alcohol was used. The HF concentration was changed in the range of 10 wt.% to 45 wt.%. Anodic current was supplied by a constant current source to maintain accurate anodic charge. The anodisation was car-

*e-mail: lukasiak@phys.uni.torun.pl

ried out in the electrolytic cell (designed for the large wafer) with backside compartment filled with NaCl solution, to get a good electrical contact with the wafer. The wafer was mounted at the wall of the cell and sealed by means of o'rings. A coiled Pt wire was used as the cathode. Such a construction assures almost uniform current density distribution over whole large wafer.

Photoluminescence excitation spectra (PLE) and photoluminescence emission spectra (PL) were registered using halogen lamp (250 W) as a source of excitation. Energies of excitation and observation were selected by two monochromators (SPM2 ZEISS with quartz prism Si68). Signal was registered by photomultiplier (9804B EMI or R-928 HAMAMATSU) using photon counting method. During time-resolved PL experiments samples were excited by a pulse nitrogen laser λ = 337.1 nm, FWHM = 3 ns, power in pulse 20 kW, 10 Hz repetition rate. Intensity of laser illumination was strongly decreased by slit and glass filter. The proper band of emission was selected by a monochromator (SPM-2 ZEISS) and registered by a combination of photomultiplier (R-928 HAMAMATSU) and boxcar. Two types of boxcar were used: analogue 162/164 PAR – for TRS in microsecond and home made digital boxcar for PL-DC in nanosecond range. Our measurements were limited by the time constant of the sampling head τ_{SH}; 0.5 μs for analogue and 10 ns for digital boxcar, respectively. Both experiments, steady-state and pulsed operation, were carried out at different temperatures (from 10 K to 300 K) and samples were enclosed in helium cryostat in vacuum environment. The signals were processed and analysed by a personal computer. Parameters of the presented multiexponential and multigaussian decompositions were recovered by an iterative fitting procedure using a nonlinear least squares search based on the Marquardt routine [8,9]. For each PSi sample the multigaussian model were applied globally to all collected PL-TRS. The centres and σ parameters of gaussian peaks were linked throughout the data sets.

3. Results and discussion

Theoretical studies of band structure of silicon nanocrystallites [4,10] in diameter range 2–4 nm (that are typical of high porosity luminescent PSi layers [11]) shows that maximum of the absorption band of such nanoparticles lies in UV part (~3–5 eV typically) of spectrum above their calculated one-electron band placed usually in visible region. Moreover, for irregular shapes of nanoparticles (characteristic of PSi prepared by electrochemical etching), mentioned absorption band may be very broad and structureless. These phenomena may be clearly observed in Fig. 1 that includes representative of our samples PL and PLE spectra at selected temperatures and energies of excitation (PL) or observation (PLE) plotted both together. There has been noticed multiband structure of PL emission spectra and blue shift of both PL and PLE with decreasing temperature. Such behaviour supports reported previously quantum confinement model of PL in PSi structures 3,5,12]. Multiband structure of emission spectrum has been observed for all our PSi samples under steady state and pulsed operation.

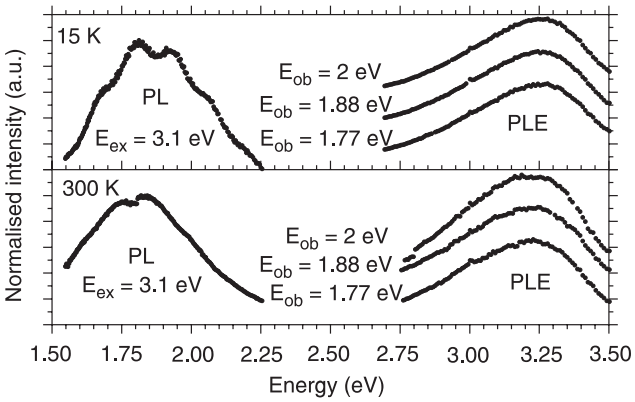

Fig. 1. Normalised photoluminescence emission (PL) spectra (the left part) and photoluminescence excitation (PLE) spectra (right part) of example porous silicon sample taken under steady state conditions at selected temperatures (15 K and 300 K). Energy of the excitation for PL was 3.1 eV, energies of observation for PLE were 2, 1.88 and 1.77 eV from top to down, respectively.

Time-resolved experiments were carried out at different temperatures (from 10 K to room temperature). PL-TRS spectra have been obtained at selected delays after laser pulse at each selected temperature. Exemplary representative results of PL-TRS measurements at room temperature are in Fig. 2. Based on the mentioned quantum confinement model that assumes radiative recombination of excited carriers inside quantum well regions of PSi skeleton formed due to interconnected different size crystallites and quantum wires with undulating diameter, we have decom-

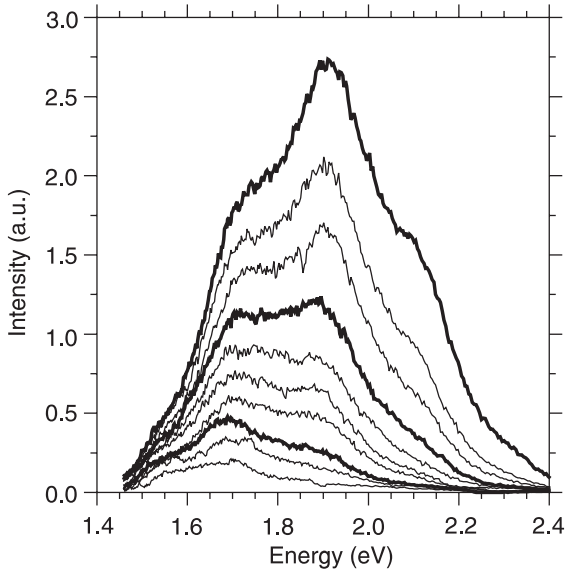

Fig. 2. Time-resolved spectra of porous silicon sample at room temperature at different delays after laser pulse: 0, 5, 10, 20, 30, 40, 50, 75, 100, and 150 μs from top to down, respectively.

posed PL-TRS as a sum of few gaussians. Number of peaks found depends on the sample (preparation conditions, porosity) but for selected PSi layer PL-TRS measured at given temperature remains constant and positions of gaussians on energy scale are independent on delay (Fig. 3). These behaviours of PL-TRS confirm our predictions because energy of radiative transitions depends only on shape and diameters of nanostructures (at constant temperature). Gaussian shape and relative broadening of peaks are due to distribution of aforesaid dimensions [11] and small distances between nanocrystallites that leads to formation of bands inside well regions (similarly to superlattices or multi quantum well systems produced by MBE methods).

Multigaussian fit applied globally to whole collection of PL-TRS for given sample gave basis to study of thermal dependence of emission energies that can be described in simple effective mass approximation by

$$\hbar\omega_i = E_{gSi} + \Delta E_{QC} - \Delta E_r, \qquad (1)$$

where $\hbar\omega_i$ is the energy of transition connected to centre of emission band numbered by i, E_{gSi} is the bandgap of bulk Si, ΔE_{QC} is the increase in energy due to quantum confinement, ΔE_r is the reduction due to excitonic and phonon related effects. Equation (1) leads to conclusion that the thermal dependence of $\hbar\omega_i$ is mainly determined by $E_{gSi}(T)$ described by semi empirical Varshni formula

$$E_{gSi}(T) = E_{gSi}(0) - \frac{\alpha T^2}{T + \beta} \qquad (2)$$

where $E_{gSi}(0) = 1.16$ eV, $\alpha = 7.02\times10^{-5}$, $\beta = 1.108\times10^{3}$ [13]. That can be because ΔE_{QC} is described by widely accepted empirical thermal independent "d^{-n}" law [14]. Reported for PSi ΔE_r is small and seems to be temperature independent too or such behaviour may be neglected [14]. Blue shift of photoluminescence of PSi from Figs. 2 and 3 is presented in Fig. 4, where gaussian-decomposed pulse coincident PL-TRS at room and 10 K, found centre positions of emission bands and calculated from Eq. 2 fits are plotted. The temperature dependence of peak positions exhibits good agreement with thermal profile of bulk Si for higher temperatures, but for some peaks at low temperatures the data do not follow monotonic variation of Eq. 2. Similar behaviour has been previously observed [15] in other quantum structures: AlGaN/InGaN/GaN, InGaAs-InP, GaInAs/AlInAs, superlattices of ZnSeMgS, GaAs/AlAs, and GaN/AlGaN. This anomalous emission characteristics has been attributed [15] to the presence of density of states which is due to a certain degree of disorder occurring mainly at interfaces (surface of PSi skeleton), which may be of compositional and structural origin.

PL-TRS study gives only quantitative information about decay rates distribution and more qualitative are PL-DC measurements. The PL-DC study was conducted in 10–297 K temperature range at different energies of the observation. Time steps were selected individually (from 10 ns to 2 ms) for each curve depended on dynamics of the PL signal (tested using LeCroy oscilloscope working in 1 GHz real-time mode). It was found that multiexponential model of decay exhibits good agreement with all obtained PL-DCs. Recovered recombination rates depend on energy of the observation and temperature. For PL-DCs registered at higher temperatures (above 50 K), decay times were

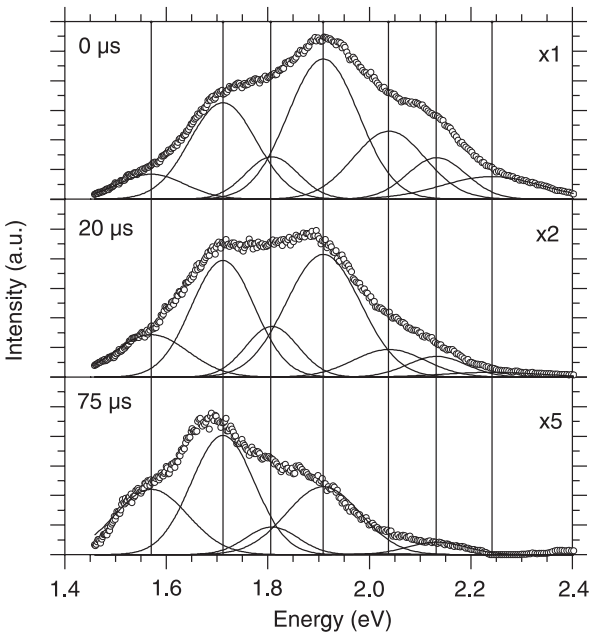

Fig. 3. Examples of multigaussian fit of selected PL-TRS from Fig. 2. Spectra at 20 µs and 75 µs were magnified (compare to pulse-simultaneous spectrum) by factor 2 and 5, respectively.

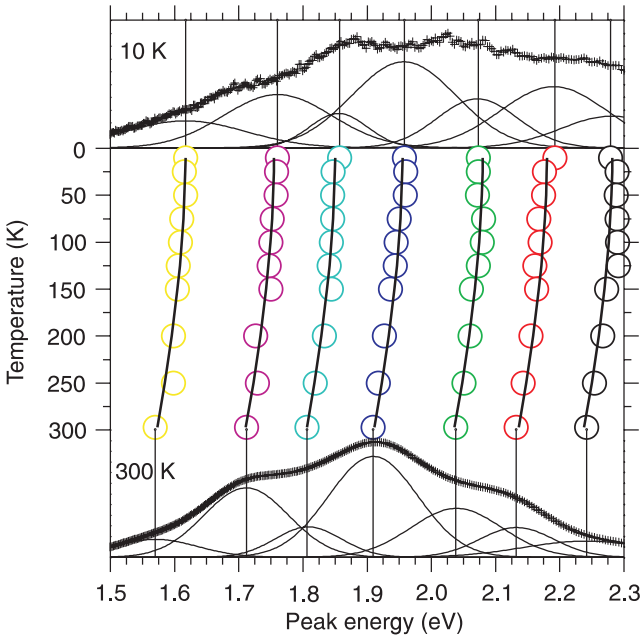

Fig. 4. Centre positions (circles) of the gaussians and profile of the energy gap of the bulk silicon (from Eq. 2 – lines) as a function of temperature. PL-TRS at 10 K and 300 K of PSi sample from Figs. 2 and 3 with results of multigaussian fits are on the top and bottom.

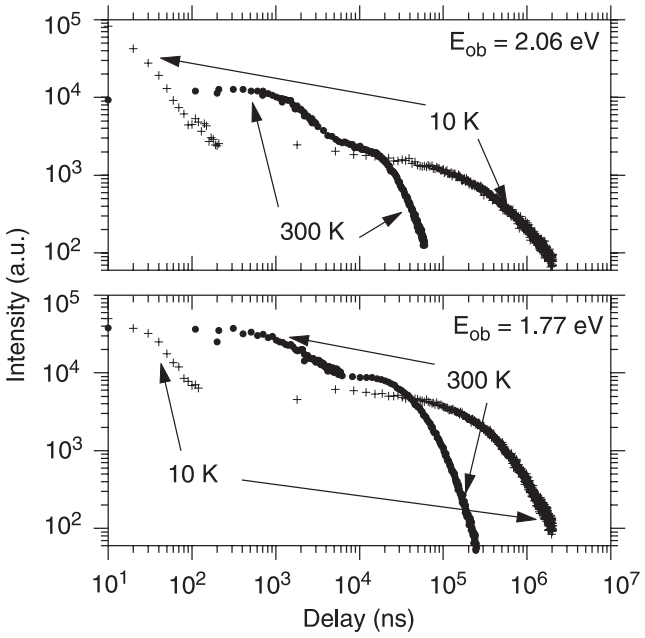

Fig. 5. Typical PL-DC of porous silicon samples measured at 10 K and 300 K, at different energy of the observation (2.06 eV – top and 1.77 eV– bottom).

found in microsecond range – no faster than 1 μs and no slower than 100 μs. At low temperatures two new behaviours have been observed. First with decay time longer than 500 μs and second very short decay in nanosecond range (which probably comes from rising probability of Auger nonradiative recombination at low temperature [12]). Selected typical PL-DC of our porous silicon samples measured at 10 K and 300 K, at different energy of the observation are presented in Fig. 5 on log-log scale to emphasize components with recombination rates at different ranges.

To discover which processes (radiative or nonradiative recombination) are dominating at given temperature and influence recombination rates, both intensity and lifetime thermal dependencies have to be considered. As it may be seen in Fig. 6, temporal behaviour of the PL can be divided into two regimes, a high temperature (HT) regime where variation in the decay time and PL intensity is the same and low temperature (LT) regime where lifetime continue increasing with fall of temperature but intensity is reduced after reaching the maximum. The temperature, at which the intensity maximum occurs, depends on a sample (porosity, passivation etc.). As the temperature is raised above that maximum, the decay time and intensity decrease together, indicating that HT regime is dominated by nonradiative recombination. This conclusion is consistent with the reports [12,14] of exponential dependence of recombination rate at room temperature which have been explained by the model proposed by Vial *et al*. [16]. The Vial model supposes that probability of finding nonradiative centres inside or on surface of nanocrystallite is small due to small volumes and surface areas. Nonradiative recombination occurs when excited carriers escape by tunnelling from small crystallites to more extended or less passivated regions of PSi skeleton. This explains relatively slow recombination rates at HT region (in comparison with those observed in bulk materials). Below the intensity maximum, the decay time increases strongly while the intensity is only weakly temperature dependent, indicating that variation in radiative processes dominates over slower nonradiative decays. The form of the variation of lifetime in LT regime can be explained by assumption of enhanced exchange interaction for excitons confined to quantum dots (nancrystallites) which causes a large excitonic splitting into triplet and singlet states. Hence, the decay time reflects the excitonic thermalisation in these two states. Assuming Boltzmann distribution between these states, the temperature-dependent radiative decay rate W_R is given by equation

$$W_R = \frac{3W_T + W_s \exp\left(-\frac{\Delta}{kT}\right)}{3 + \exp\left(-\frac{\Delta}{kT}\right)}, \tag{3}$$

where W_T, W_S are the radiative decay rates of triplet and singlet excitons, respectively, k is the Boltzmann constant, Δ is the triplet-singlet energy splitting.

In the singlet state dipole-allowed radiative transition is fast, while in the triplet dipole-prohibited is slow. At low temperature, all the luminescence comes from the lower slow state (kT at $T < 10$ K is negligible compared with Δ), but when the temperature is increased also the fast upper state becomes populated and the lifetime decreases. The termalisation of excitons between singlet and triplet states also explains thermal dependence of PL intensity. In fact,

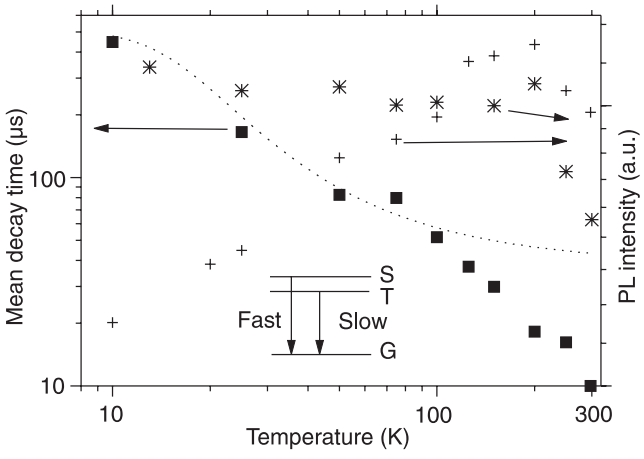

Fig. 6. Log-log plot of simultaneously recorded temperature dependencies of the lifetime (black squares) and intensity of luminescence detected at 650 nm (crosses) under pulsed operation. Stars represent integrated intensity of PL recorded under steady state conditions. Dot line – radiative recombination rate calculated from Eq. 3, using values $\Delta = 10$ meV, $W_S = 10^5$ s^{-1}, $W_T = 2\times10^3$ s^{-1} taken from Ref. 12. Inset: energy level diagram for an exciton having an excited state split and with fast and slow radiative rates from two components (S – singlet, T – triplet, G – ground state).

at LT mostly triplet state luminescence is observed which has a low efficiency, while raising the temperature the singlet state luminescence overcomes and intensity increases. For steady state integrated PL intensity (Fig. 6 – stars) effect is smaller than for pulse excited PL due to saturation processes in the first case.

4. Conclusions

Large Stokes shift observed in the PLE and PL results suggests that the luminescent emission primary occurs via relaxed electronic states, i.e., the states that have the largest absorptive oscillator strength are not the states through which the photoexcited electron-hole pairs radiatively recombine. Blue shift of PL (and PL-TRS) spectra described by Varshni formula for bulk Si corrected by confinement energy supports that prediction. Temperature variation of PL decay time and intensity is naturally explained by quantum confinement model. At high temperature nonradiative recombination occurs by escape (tunnelling) carriers from nanocrystallites to extended regions of skeleton where probability of existing nonradiative trap is higher. At low temperature radiative recombination dominates and model of two singlet-triplet exciton states explain long decay time and decreasing PL intensity.

Acknowledgements

This work is partially supported by the N. Copernicus Univ. Scientific Research – project No. 376-F.

References

1. L. Esaki and R. Tsu, *IBM J. Res. Develop.* **14**, 61 (1970).
2. L.T. Canham, "Silicon quantum wire array fabrication by electrochemical and chemical dissolution of wafers", *Appl. Phys. Lett.* **57**, 1046–1048 (1990).
3. W. Bała, G. Głowacki, Z. Łukasiak, M. Drozdowski, M. Kozielski, E. Nossarzewska-Orłowska, and A. Brzozowski, "Photoluminescence, reflectivity and Raman investigations of nanocrystallites in luminescent porous silicon", *Acta Phys. Polon.* **A87**, 445–448 (1995).
4. J.P. Proot, C. Delerue, and G. Allen, "Electronic structure and optical properties of silicon crystallites: application to porous silicon", *Appl. Phys. Lett.* **61**, 1948–1050 (1992).
5. Z. Łukasiak, Z. Wyrzykowski, J. Sylwisty, and W. Bała, "Influence of gas adsorption on photoluminescence properties of porous silicon layers", *Electron Technology* **33**, 207–209 (2000).
6. L. Seals and J.L. Gole, "Rapid, reversible, sensitive porous silicon gas sensor", *J. Appl. Phys.* **91**, 2519–2523 (2002).
7. G. Belomoin, J. Therrien, A. Smith, S. Rao, R. Twesten, S. Chaieb, M.H. Nayfeh, L. Wagner, and L. Mitas, "Observation of magic discrete family of ultrabright Si nanoparticles", *Appl. Phys. Lett.* **80**, 841–843 (2002).
8. P.R. Bevington, *Data Reduction and Error Analysis for the Physical Sciences*, pp. 204–246, McGraw Hill, NY, 1969.
9. D. Marquardt, "An algorithm for least-squares estimation of nonlinear parameters", *J. Soc. Indust. Appl. Math.* **11**, 431–441 (1963).
10. M. Lannoo, G. Allan, and C. Delerue, *Structural and Optical Properties of Porous Silicon Nanostructures*, p. 187, edited by G. Amato, C. Delerue, H.J. von Bardeleben, Gordon and Breach, Amsterdam, 1997.
11. R.J. Martin-Palma, L. Pascual, P. Herrero, and J.M. Martinez-Duart, "Direct determination of grain sizes, lattice parameters, and mismatch of porous silicon", *Appl. Phys. Lett.* **81**, 25–27 (2002).
12. Z. Łukasiak, M. Murawski, and W. Bała, "Photoluminescence of porous silicon under pulsed excitation", *SPIE* **4413**, 157–162 (2001).
13. J. Porębski and P. Kohoroda, "*Spice – a program of nonlinear analysis of electronic systems*", p. 89, Wydawnictwa Naukowo-Techniczne, Warsaw, 1995. (in Polish)
14. O. Bisi, S. Ossicini, and L. Pavesi, "Porous silicon: a quantum sponge structure for silicon based optoelectronics", *Surface Sci. Rep.* **38**, 1–126 (2000).
15. L. Bergman, M. Dutta, M. Stroscio, S. Komirenko, R. Nemanich, C. Eiting, D. Lambert, H. Kwon, and R. Dupuis, "Photo-luminescence and recombination mechanisms in GaN/AlGaN superlattice", *Appl. Phys. Lett.* **76**, 1969–1971 (2000).
16. J.C. Vial, A. Bsiesy, F. Gaspard, R. Herino, M. Ligeon, F. Muller, and R. Romestain, "Mechanisms of visible light emission from electro-oxidized porous silicon", *Phys. Rev.* **B45**, 14171–14176 (1992).

7th International Workshop on Advanced Infrared Technology and Applications AITA 2003

September 9–11, 2003
Scuola Normale Superiore Pisa, Italy
http://ronchi.iei.pi.cnr.it/AITA2003

The International Workshop on 'Advanced Infrared Technology and Applications' (AITA) is the seventh event of a series started in 1991. AITA constitutes a forum bringing together academic and industrial researchers to exchange knowledge, ideas and experiences in the field of infrared science and technology.

Chairman
L. Ronchi Abbozzo

Co-chairmen
G.M. Carlomagno, C. Corsi, E. Grinzato, I. Pippi, N.H. Rutt, O. Salvetti

Scientific Committee
D. Balageas, ONERA, Chatillon, France
J.M. Buchlin, VKI, Rhode-Saint-Genèse, Belgium
C.T. Elliott, Heriot-Watt University, Edinburgh, Scotland.
X. Maldague, Laval University, Quebec, Canada
E. Paganini, ENEL Produzione Spa, Pisa, Italy
A. Rogalski, Institute of Applied Physics, Warsaw, Poland
T. Sakagami, Osaka University, Japan
M. Strojnik, CIO, Leon Gto, Mexico
J.L. Tissot, ULIS, Veurey Voroize, France
V.P. Vavilov, Tomsk University, Russia
H. Wiggenhauser, BAM, Berlin, Germany
H. Zogg, ETH, Zurich, Switzerland

Topics
- Advanced technology and materials
- Smart sensors
- Thermofluid dynamics
- Far infrared
- Non-Destructive Evaluation
- Image processing and data analysis
- Advanced systems in cultural heritage, biomedicine, environment, aerospace, etc.
- Industrial applications

Abstracts Submission Guidelines
Submit a 300-500 words abstract electronically within March 15, 2003, indicating clearly title, name and affiliation of the Authors and the topic. Address, phone, fax number and E-mail of the corresponding Author must be also specified. Abstracts can be mailed to *AITA2003@isti.cnr.i*t or submitted via Web (*http://ronchi.iei.pi.cnr.it/AITA2003*).

Deadlines
- March 15, 2003 — Abstract submission
- April 30, 2003 — Papers acceptance notification
- July 15, 2003 — Final program delivery

Registration fees
- Euro 300, regular registration including: Social dinner, Coffee-breaks, Lunch, Abstracts and Proceedings
- Euro 150, student registration including: Coffee-breaks, Lunch and Abstracts

Publication
A book of abstracts of the accepted papers will be available at the workshop. Authors are also requested to deliver their contributions directly at the registration desk for proceedings publication. Furthermore, selected papers will be published in an international journal.

Language
English is the official language of the Workshop. All papers should be written and presented in English.

Technical Secretariat
Anna M. Meriggi
Fondazione Giorgio Ronchi
Via S. Felice a Ema, 20
50125 Firenze, Italy
Tel./Fax: +39 055 2320844
E-mail: *ronchi@infinito.it*

Organizing Secretariat
Ettore Ricciardi
CNR-ISTI, Via G. Moruzzi, 1
56124 Pisa, Italy
Tel.: +39 050 315 2907
Fax: +39 050 315 2810
E-mail: *ricciardi@iei.pi.cnr.it*

